Crystal phase induced direct band-gap modifications in bulk GaP and GaAsP

N. Benyahia, A. Menad, Ali Zaoui, M. Ferhat

Version of Record: https://www.sciencedirect.com/science/article/pii/S0038109821003689
Manuscript_b35034dd34b466894f5f941788322c3a

Crystal phase induced direct band-gap modifications in bulk GaP and GaAsP

N. Benyahia[1], A. Menad[1], A. Zaoui[2,*] and M. Ferhat[1]

[1]*Département de Génie Physique, (LPMF). Université des Sciences et de la Technologie d'Oran, Mohamed Boudiaf. Oran, Algeria*

[2]*Univ. Lille, IMT Lille Douai, Univ. Artois, JUNIA, ULR 4515 - LGCgE, Laboratoire de Génie Civil et géo-Environnement, F-59000 Lille, France*

Abstract

Wurtzite III-phosphide GaP and GaAsP compounds have shown tunable direct band-gap making them promising candidates in a variety of future optoelectronic and photonic devices. We explore here, through DFT their corresponding electronic structure properties of bulk cubic and wurtzite polytypes. It is shown that the calculated weak positive formation enthalpy of GaAsP crystal-phases suggest slight thermodynamical instability. In addition, from accurate quasiparticle (local density approximation-1/2) we predict a direct band-gap for WZ 2H, 4H, and 6H polytypes of GaP and GaAsP. The emitted wavelength can be then tuned across an important range of the visible light yellow-green spectrum for GaP (2.13eV(2H)-2.33eV(4H)) and the visible light red spectrum for GaAsP (1.64eV(6H) to 1.82eV(4H)).

Keywords: GaAsP; DFT; structural stability; thermodynamic stability; band structure.

*Email address: azaoui@polytech-lille.fr

III-V semiconductors nanowires (Nws) [1-2], the emerging of ideal building components of novel nanoscale devices, have recently attracted important attention due to the fascinating fundamental investigations and unprecedented potential technological application that these Nws enable.

III-V Nws typically show polytypism that is the intermixing of cubic zinc-blende (ZB) and hexagonal wurtzite (WZ) crystal phases. Indeed, the WZ structure is often absent in bulk non-nitrides III-V compounds; while it can be obtained in NWs. Interestingly, Nws can be easily switched between these phases by varying the temperature and growth conditions.

The resulting change of atomic stacking sequence (i.e., WZ vs ZB crystal phases) impacts considerably the transport and the optical properties, which creates strong opportunities for designing modulate nanowire structures with new electronic properties, and to extend band structure engineering.

Of particular interest is gallium phosphide (GaP) with an indirect gap of 2.3eV, in spite of the fact that GaP has the smallest lattice mismatch to Si, and it is therefore one of the best candidates for integration of optoelectronic and photonic based on III-V materials. However cubic-GaP has indirect band gap, which results in a low radiative efficiency and requires a relatively large absorption depth.

Recently, GaP nanowire with WZ structure has been successfully grown by vapor-liquid-solid (VLS) mechanism [3-6], Au chemical beam epitaxy (CBE) [7], and molecular-beam epitaxy (MBE) [8]. Photoluminescence excitation spectroscopy (PLE) demonstrates the conversion of the indirect nature of the band-gap of bulk-ZB-GaP to a NWs-WZ direct band-gap of 2.09-2.11eV [4] and ~ 2.19eV [6]; whereas resonance Raman (RR) spectroscopy measurements give a higher direct band-gap of 2.47eV [7]. In addition, it was demonstrated experimentally that by the incorporation of arsenic (As) in GaP Nws, the emitted wavelength is tuned across an important range of the visible light spectrum [9], since its band-gap can be tuned from the

near-infrared (E_g = 1.42eV, λ = 873.12 nm) to visible region (Eg = 2.3eV, λ = 539.06nm). Moreover, GaAsP NWs systems have great potential for light emitting diodes, optoelectronic and photovoltaics applications.

In view of the above, and despite the numerous above-mentioned advantages of GaP, many questions remain unaddressed regarding the doping effects of As on the electronic-structure properties of WZ GaP. Knowledge on the material properties of the bulk phase of GaAs/GaP materials is the first step towards the optimization of device performances and the design of new Nws-based devices. Moreover, the knowledge about the electronic structure properties of WZ-GaAsP systems is quite limited in the literature.

Herein, we explore the structure, and electronic properties of cubic and wurtzite 2H, 4H and 6H bulk form of GaAs/GaP systems by applying the state-of-the-art first-principles pseudopotential calculations.

Calculations have been performed within the framework of the density functional theory (DFT) [10], as implemented in the *ab initio* plane-wave pseudopotential Quantum ESPRESSO code [11]. The projector-augmented wave pseudopotential (PAW) [12] was used to represent the ion-electron interaction. The local density approximation (LDA)[13] is used to describe the exchange and correlation potentials. Single-particle Kohn-Sham wave function was extended using the plane wave with cutoff energy of 60Ry along a cutoff of 500Ry for the augmentation charges. A convergence test was done before handling the main parts of the work. It confirms the value used is widely enough to ensure the convergence. For GaAsP systems we used cubic supercell of GaP (8 atoms), and WZ supercells of GaP 2H (8 atoms), 4H(8 atoms) and 6H (24 atoms) by replacing one As atom with one P atom. A Monkhorst-Pack [MP] [14] *k*-points sampling of: 4×4×4(cubic), 4×4×3(2H), 4×4×2(4H), and 4×4×2(6H) were employed to sample the Brillouin zone. A convergence test was achieved in

order to confirm the number of k-points necessary to accomplish each study. These settings ensure energy convergence within 10^{-4}eV/cell. Atomic degrees of freedom are relaxed until the maximum forces on all atoms had fallen below 10^{-5}eV/Å.

The energy equilibrium structural parameters of the 3C(ZB-phase), 2H, 4H and 6H polytypes of GaP, GaAs and the cubic, 2H, 4H and 6H polytypes of GaAsP systems are obtained by minimizing the total energy with respect to the lattice constants (*a*, and *c*) and the structural parameter *u*. The minimum of the total energy *E*=*E*(*a*,*c*) (Fig.1, for GaAsP systems) is then derived for the equilibrium a_{eq}, c_{eq} together with the corresponding internal-cell parameters. For the cubic phase (GaAsP) and 3C (GaP and GaAs) phase only the lattice constant *a* has to be optimized.

The results of the structural optimization for GaAs, GaP and GaAsP compounds are given in Table I for the four polytypes. The polytypes are ordered according to their hexagonality *H* defined as the fraction of the number of the hexagonal bilayers to the total number of bilayers per unit cell: $H = \frac{h}{h+c}$

where *h* and *c* are the number of hexagonal and cubic stacking respectively. Between the most extreme polytype 2H with *H*=100 % and 3C (Only for GaP and GaAs) with *H*=0, one finds the intermediate hexagonal polytypes 4H (*H*=50%) and 6H (*H*=33 %).

Experimental data of the structure properties of WZ polytypes of GaP and GaAs are generally not available. However, recently, structural characterization of WZ GaP and GaAs Nws was obtained [15]. The present calculated equilibrium lattice parameters *a* and *c* of 2H-GaP are in excellent agreement with X-ray diffraction data [15], the deviation do not exceed ~ 1% for *a* and ~ 0.1% for *c*. Moreover, the X-ray diffraction measurements [16] of the ratio interplanar spacing $\frac{d_{WZ}}{d_{ZB}} \sim 1.60$ of GaAs nanowires agree perfectly with our calculated value of 1.60.

The *c*/*a* ratio increases with increasing hexagonality *H*, for GaP, GaAs and GaAsP systems, which corresponds to an increasing deformation of the bonding tetrahedra that are stretched along the *c* axis. The lattice constant *a* decreases with rising hexagonality and exhibits a minimum for 4H polytype only for GaAsP systems. In contrast, the bulk modulus of GaP, GaAs and GaAsP materials show a very weak dependence on the polytype.

The physical properties as indicator of the possibility of synthesis of GaAsP systems is the formation energy ΔH, which describes the energy required to from the GaP-GaAs systems with respect to the ZB binary GaP and GaAs. The calculated ΔH for the cubic and WZ 6H, 4H and 2H polytypes are respectively 8.54meV/pair, 35.87meV/pair, 46.22 meV/pair and 95.06 meV/pair. The calculated enthalpy of formation for the four phases is in the order: $E(2H) > E(4H) > E(6H) > E(\text{cubic})$. The WZ polytypes are found energetically less stable than the cubic crystal. In all cases we found $\Delta H > 0$, which suggests phase separation into the binary GaAs and GaP. However, ΔH is found extremely small, suggesting that the GaAsP crystals are thermodynamically slightly unstable.

To gain better insight into the physical factors controlling ΔH, we decompose the total formation energy $\Delta H = \Delta H\,(\text{Chem}) + \Delta H\,(\text{Elast})$ into 'chemical' (Chem) and 'elastic' (Elast) parts. For the cubic crystal for example, the calculated ΔH (Chem) and ΔH (Elast) are respectively 7.64meV/pair and 0.90 meV/pair. The calculated ΔH (Chem) and ΔH (Elast) show that chemical energy part is the main contribution to ΔH. Moreover, the excessively small ΔH (Chem) and ΔH (Elast) can be correlated to the small lattice parameter mismatch ($\frac{\Delta a}{a} \sim 4\%$) between the binary GaAs and GaP and with the low electronegativity mismatch between As and P (i.e., χ(P)-χ(As) ~0.01 within the Pauling scale [17]).

Indeed, various GaAsP Nws have been successfully synthesized recently. Cubic Nws have been synthesized by molecular beam epitaxy (MBE) [18], WZ-Nws of GaAsP compounds were grown by Aerotaxy technique [19], by MBE [20-22], by Au-assisted vapor-liquid-solid (VLS) [3] growth mode, and by vapor transport method [23].

The four studied cubic-wurtzite polytypes of GaAs/GaP systems considered here can be reasonably described by one-dimensional Ising-type model, more precisely the axial next-nearest-neighbor Ising (ANNNI) model [24]. Within the ANNNI model we can compute the parameters J_i, which describe the interaction energy between neighbor layers. We restrict the J_i up to the third-neighbor bilayers (i.e., J_1, J_2, and J_3). The ANNNI J_i parameters have been computed according to Ref. [25] as:

$$J_1 = \frac{\Delta E(2H)}{2} + \frac{\Delta E(4H)}{2} - 3\frac{\Delta E(6H)}{4}$$

$$J_2 = -\frac{\Delta E(2H)}{4} + \frac{\Delta E(4H)}{2}$$

$$J_3 = -\frac{\Delta E(4H)}{2} + 3\frac{\Delta E(6H)}{4}$$

Where ΔE is the total energy difference of polytype with respect to the cubic phase. The resulting layer-layer interaction energies (meV/pair) are J_1=10.40, J_2=0.69 and J_3=0.41. The nearest-neighbor interaction leads to the dominant parameter J_1. The value of J_1 has the correct order of magnitude of III-V compounds. The J_1 parameter is positive, which correlates with the cubic-wurtzite phase-preference (i.e., $J_1>0$ ($J_1<0$) favors cubic (wurtzite) crystal). The second and third-nearest neighbor interaction J_2 and J_3 are found much smaller than J_1, and valid the assumption that the long-range interaction in the polytypes considered here are small.

Important information can also be deduced from the ANNNI model in relation with the two-dimensional planar defects that can occur in crystalline materials. Given the layer-layer interaction energies one can estimate the stacking faults (SF) formation energies. The most common stacking faults are the intrinsic stacking fault (ISF), and the extrinsic stacking fault (ESF). The predicted stacking fault energies (per unit area) are γ(ESF)=50.45mJ/m^2, and γ(ISF)=49mJ/m^2. The calculated SF energies indicate that both intrinsic and extrinsic stacking faults energies are unstable.

It is well known that very often DFT-GGA seriously underestimates quasiparticles (QP) band-gap energies from the experimental ones of semiconductors and insulators, typically Kohn-Sham gap underestimates excited-states of solids by 50%-100%. Hence, we apply the LDA-1/2 technique [26] which leads to more accurate excited states, and rivals well with the results of the expensive many-body GW quasiparticle approach [27]. The QP self-energy effects are simulated by a hole excitation whose extent is derived by maximizing the fundamental energy gap of ZB GaAs and GaP.

The quasiparticle LDA-1/2 band structures of 3C and WZ polytypes (2H, 4H and 6H) of GaP are displayed in Fig. 2. We found that all WZ GaP-polytypes show a semiconductor character with a direct band gap ($\Gamma\rightarrow\Gamma$) of 2.33eV, 2.285eV and 2.138eV for 6H, 4H and 2H polytypes respectively; while the cubic phase shows indirect band-gap of ~2.39 eV at X point. The calculated 2H band gap of GaP is in excellent agreement with the measured values of 2.09-2.11eV [4] and 2.19eV [6]. Whereas the directness nature of the band gap of GaP is found rather independent with WZ-polytypes, the strength of the direct gap is found dependent of the crystal phase that can adopt GaP. Fig. 5a shows the calculated direct energy gap as function of hexagonality H. E_g exhibits relatively strong dependence versus H, a fit of the curve give a band gap bowing of ~0.64eV. Our results agree with the screened exchange

LDA [28] (QP (LDA-1/2) [29]) calculations for the direct nature of the band-gap of 2H(2.12eV)[29], and 4H(2.26eV)[29] WZ polytypes of GaP.

Considering now QP band structures of GaAs (Figure 3), all polytypes are found direct semiconductors. QP(LDA-1/2) calculations support our findings [29]. The variation of the direct band gap of GaAs versus hexagonality *H* (Fig.5c) expresses insignificant dependence. We predict a direct band gap of ~1.43 eV for 2H GaAs in very good agreement with the measured values of 1.46eV [30] and 1.444 eV [31].

The electronic LDA-1/2 band structures for cubic and WZ polytypes of GaAsP systems are presented in Fig. 4. The computed minimum LDA-1/2 band-gap of 2H, 4H and 6H polytypes of GaAsP systems are respectively 1.7eV, 1.82eV, and 1.64eV. We notice here that all those band-gaps are direct along $\Gamma\rightarrow\Gamma$ direction (E_g(D)). In addition, indirect E_g(I) ($\Gamma\rightarrow$A) band gap is close to the $\Gamma\rightarrow\Gamma$ optical transitions. E_g(D) is comparable to E_g(I) to within ~0.01eV, ~0.002eV, ~0.05eV, and ~0.08eV for the cubic, and WZ 6H, 4H and 2H polytypes respectively. The cubic phase divulges indirect nature of the band gap at the *R* point (E_g(I)~2.23eV). The evolution of E_g(D) versus the stacking sequence is given in Fig. 5b. E_g(D) evinces relative weak dependence versus *H*. Interestingly, as found for WZ-polytypes of GaP, the direct nature of the band-gap for GaAs/GaP systems is preserved for all WZ polytypes. Moreover, the gap energy with direct transition in WZ polytypes of GaAsP, is ranging from 1.64eV(λ=756nm)(6H) to 1.82eV(λ = 681.23nm)(4H), suggesting that the emission wavelength can be tuned across the visible-red light spectrum.

To conclude, using the state-of-the-art first principles DFT theory within plane-wave pseudopotential method, we have investigated the structural energetic and electronic properties of cubic and hexagonal (2H, 4H, and 6H) polytypes of GaAsP systems. WZ

polytypes are found energetically less stable than in the cubic phase. Moreover, the calculated weak positive formation energy of cubic-WZ polytypes of GaAsP compounds suggests relative weak thermodynamic instability. The results show excellent agreement with the available experimental measurements for structural parameters and band gaps for WZ polytypes of GaP and GaAs. Using the one-dimensional Ising-type (ANNNI) model we have also determined the layer-layer interaction and stacking fault energies of GaAsP materials. Most importantly, QP(LDA-1/2) band structure of WZ GaAsP systems evidence direct band semiconductor behavior with gap energies of 1.64eV(6H), 1.82eV(4H), and 1.7eV(2H), which are promising candidates for light emission across an important range of visible light spectrum.

References

[1] W. Lu and C. M. Lieber, Nat. Mater. **6**, 841 (2007).

[2] P. Yang, R. Yan, and M Fardy, Nano Lett. **10**, 1529 (2010).

[3] J. P. Boulanger, and R. R. LaPierre, J. of Crystal Growth **332**, 21 (2011).

[4] S. Assali, I. Zardo, S. Plissard, D. Kriegner, M. A. Verheijen, G. Bauer, A. Meijerink, A. Belabbes, F. Bechstedt, J. E. M. Haverkort, and E. P. A. M. Bakkers, Nano Lett. **13**, 1559 (2013).

[5] A. Dobrovolsky, S. Sukrittanon, Y. J. Kuang, C. W. Tu, W. M. Chen, and I. A. Buyanova, Appl. Phys. Lett. **105**, 193102 (2014).

[6] B. C. da Silva, O. D. D. Coutou Jr., H. T. Obata, M. M. de Lima, F. D. Bonani, C. E. de Oliveira, G. M. Sipahi, F. likawa, and M. A. Cotta, Sci. Rep. **10**, 7904 (2020).

[7] J. K. Panda, A. Roy, M. Gemmi, E. Husanu, A. Li, D. Ercolani, and L. Sorba, Appl. Phys. Lett. **103**, 023108 (2013).

[8] A. D. Bolshakov, V. V. Fedorov, N. V. Sibirev, M. V. Fetisova, E. I. Moiseev, N. V. Kryzhanovskaya, O. Yu. Koval, E. V. Ubyivovk, A. M. Mozharov, G. E. Cirlin and I. S. Mukhin, Phys. Status Solidi RRL 13, 1900350 (2019).

[9] M. Ghasemi, E. D. Leshchenko, and J. Johansson, Nanotechnology **32**, 072001 (2021), and references therein.

[10] P. Hohenberg and W. Kohn, Phys. Rev. **136**, B 864 (1964); W. Kohn and L. J. Sham, Phys. Rev. **140**, A1133 (1965).

[11] S. Baroni, A. Dal Corso, S. de Gorconli, and P. Giannozzi in https://www.pwscf.org.

[12] A. Dal Corso, Phys. Rev. B **82**, 075116(2010).

[13] J. P. Perdew and A. Zunger, Phys. Rev. B **23**,5048(1981).

[14] H. J. Monkhorst and J. D. Pack, Phys. Rev. B **13**, 5188 (1976).

[15] D. Kriegner, S. Assali, A. Belabbes, T. Etzelstorfer, V. Holý, T. Schülli, F. Bechstedt, E. P. A. M. Bakkers, G. Bauer, and J. Stangl, Phys. Rev. B **88**, 115315 (2013).

[16] M. Köhl, P. Schroth, A. A. Minkevitch, J.-W. Hornung, E. Dimakis, C. Somaschini, L. Geelhaar, T. Aschenbrenner, S. Lazarev, D. Grigoriev, U. Pietsch, and T. Baumbach, J. Synchrotron Rad. **22**, 67 (2015).

[17] L. Pauling, J. Am., Chem. Soc. **54**, 3570 (1932).

[18] Y. Zhang, H. A. Fonseka, M. Aagesen, J. A. Gott, A. M. Sanchez, J. Wu, D. Kim, P. Jurczak, S. Huo, and H. Liu, Nano Lett. **17**, 4946 (2017).

[19] W. Metaferia, A. R. Persson, K. Mergenthaler, F. Yang, W. Zhang, A. Yartsev, R. Wallenhberg, M.-E. Pistol, K. Deppert, L. Samuelson, and M. H. Magnusson, Nano Lett. **16**, 5701 (2016).

[20] O. D. D. Couto Jr., D. Sercombe, J. Puebla, L. Otubo, I. J. Luxmoore, M. Sich, T. J. Elliott, E. A. Chekhovich, L. R. Wilson, M. S. Skolnick, H. Y. Liu, and A. I. Tartakouskii, Nano Lett. **12**, 5269 (2012).

[21] Y. Zhang, J. Wu, M. Aagesen, J. Holm, S. Hatch, M. Tang, S. Huo and H. Liu, Nano Lett. **14**, 4542 (2014).

[22] C. Himwas, S. Collin, P. Rale, N. Chauvin, G. Patriarche, F. Oehler, F. H. Julien, L. Travers, J. –C. Harmand and M. Tchernycheva, Nanotechnology **28**, 495707(2017).

[23] H. S. Im, C. S. Jung, K. Park, D. M. Jang, Y. R. Lim, and J. Park, J. Phys. Chem. C **118**, 4546 (2014).

[24] J. von Boehm and P. Bak, Phys. Rev. Lett. **42**, 122 (1979).

[25] J. Johansson, Z. Zanolli, and K. A. Dick, Cryst. Growth Des. **16**, 371 (2016).

[26] L. G. Ferreira, M. Marques and L. K. Teles, Phys. Rev. B **78**, 125116 (2008).

[27] M. S. Hybersten, and S. G. Louie, Phys. Rev. B **37**, 2733 (1988).

[28] T. Akiyama, K. Nakamura, T. Ito, and A. J. Freeman, Appl. Phys. Lett. **104**, 132101 (2014).

[29] F. Bechstedt, and A. Belabbes, J. Phys. : Condens. Matter **25**, 273201 (2013).

[30] P. Kusch, S. Breuer, M. Ramsteiner, L. Geelhaar, H. Riechert, and S. Reich, Phys. Rev. B **86**, 075317 (2012).

[31] L. Ahtapodov, J. Todorovic, P. Olk, T. Mjåland, P. Slåttnes, D. L. Dheeraj, A. T. J. van Helvoort, B. –O. Fimland, and H. Weman, Nano Lett. **12**, 6090 (2012).

Table Captions

Table I: Structural (*a*, *c*), and Bulk modulus (B_0) of crystal structures for cubic and WZ polytypes (2H, 4H and 6H) of GaAs, GaP and GaAsP. The lattice constants are given referred to the corresponding hexagonal unit cell, i.e., $a = a_0/\sqrt{2}$ and $c = a_0/\sqrt{3}$. p is the number of bilayers per unit cell p (p=2(2H), p=4(4H), and p=6(6H)).

Table I

Material	Polytype	*a*(Å)	2*c*/(Pa)	$\boldsymbol{B_0}$**(GPa)**
GaAs	2H	3.955	1.649	73.80
	4H	3.962	1.640	73.91
	6H	3.963	1.638	73.93
	3C	3.969	1.633	74.06
GaP	2H	3.801	1.649	89.45
	4H	3.807	1.641	89.54
	6H	3.809	1.638	89.58
	3C	3.816	1.633	89.78
GaPAs	2H	3.839	1.650	85.12
	4H	3.845	1.641	85.18
	6H	3.844	1.639	86.62
	Cubic	3.853	1.633	85.6

Figure Captions

Figure 1: Isoenergies lines of the total energy $E(c, a)$ of crystal phases of GaAsP.

Figure 2: Quasiparticle (LDA-1/2) band structures of GaP polytypes.

Figure 3: Quasiparticle (LDA-1/2) band structures of GaAs polytypes.

Figure 4: Quasiparticle (LDA-1/2) band structures of GaAsP polytypes.

Figure 5: Direct band-gap evolution as function of the hexagonality H of: a) GaP, b) GaAsP and c) GaAs.

Figure 1

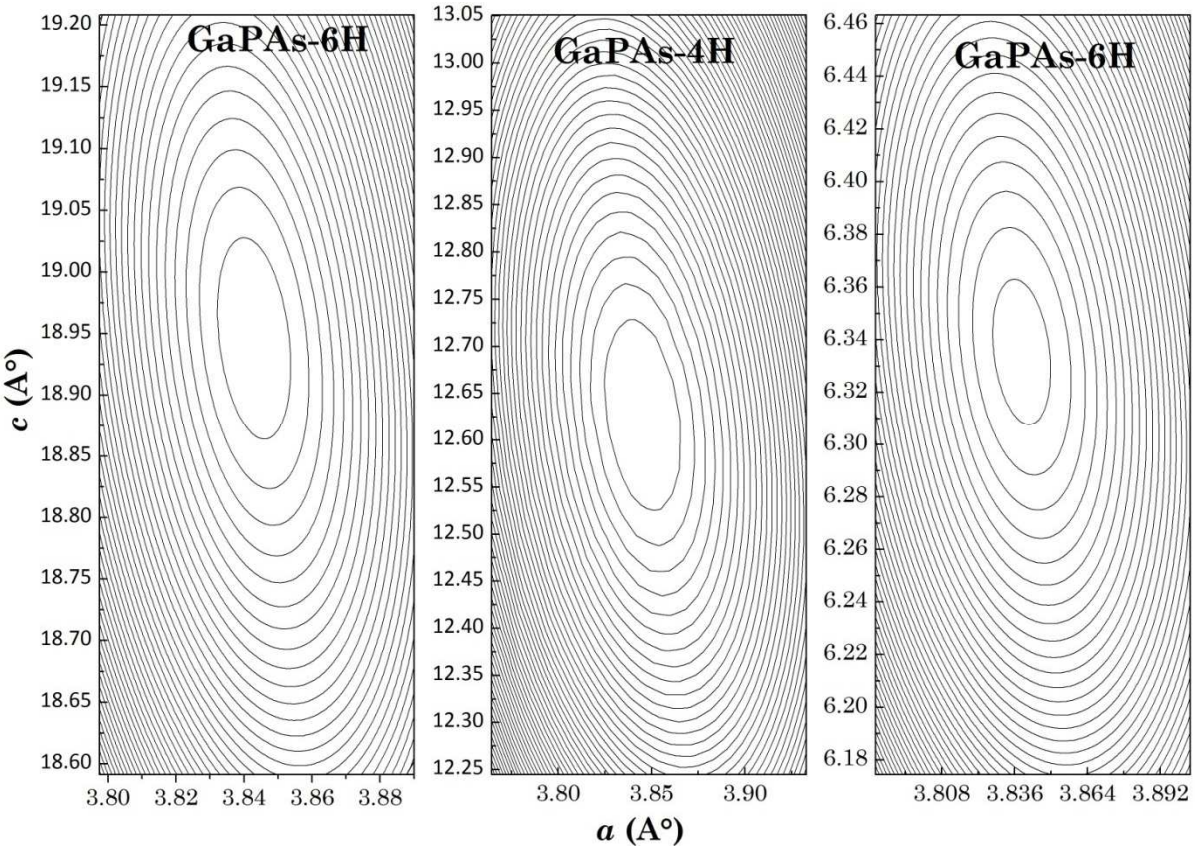
GaPAs-6H
GaPAs-4H
GaPAs-6H
c (A°)
a (A°)
19.20
19.15
19.10
19.05
19.00
18.95
18.90
18.85
18.80
18.75
18.70
18.65
18.60
3.80 3.82 3.84 3.86 3.88
13.05
13.00
12.95
12.90
12.85
12.80
12.75
12.70
12.65
12.60
12.55
12.50
12.45
12.40
12.35
12.30
12.25
3.80 3.85 3.90
6.46
6.44
6.42
6.40
6.38
6.36
6.34
6.32
6.30
6.28
6.26
6.24
6.22
6.20
6.18
3.808 3.836 3.864 3.892

Figure 2

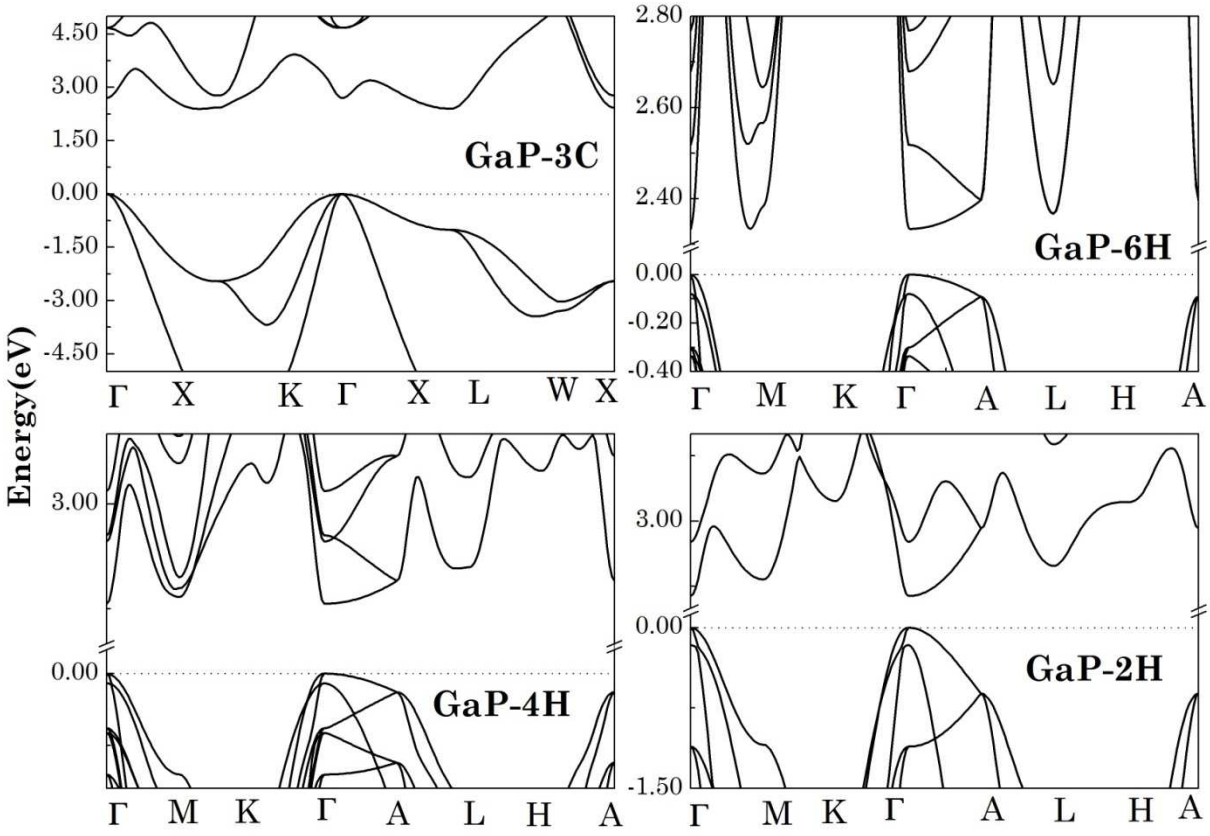
Energy(eV)
GaP-3C
4.50
3.00
1.50
0.00
-1.50
-3.00
-4.50
Γ X K Γ X L W X
GaP-6H
2.80
2.60
2.40
0.00
-0.20
-0.40
Γ M K Γ A L H A
GaP-4H
3.00
0.00
Γ M K Γ A L H A
GaP-2H
3.00
0.00
-1.50
Γ M K Γ A L H A

Figure 3

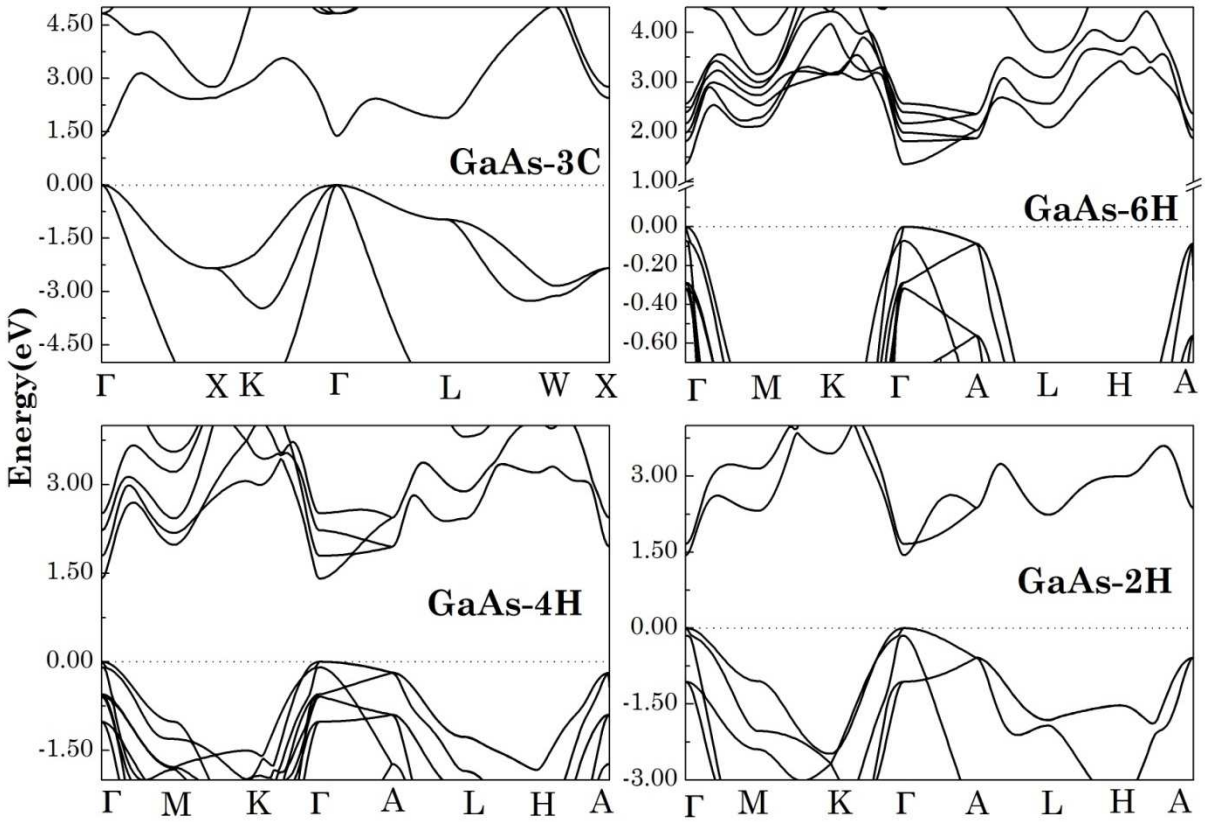

Figure 4

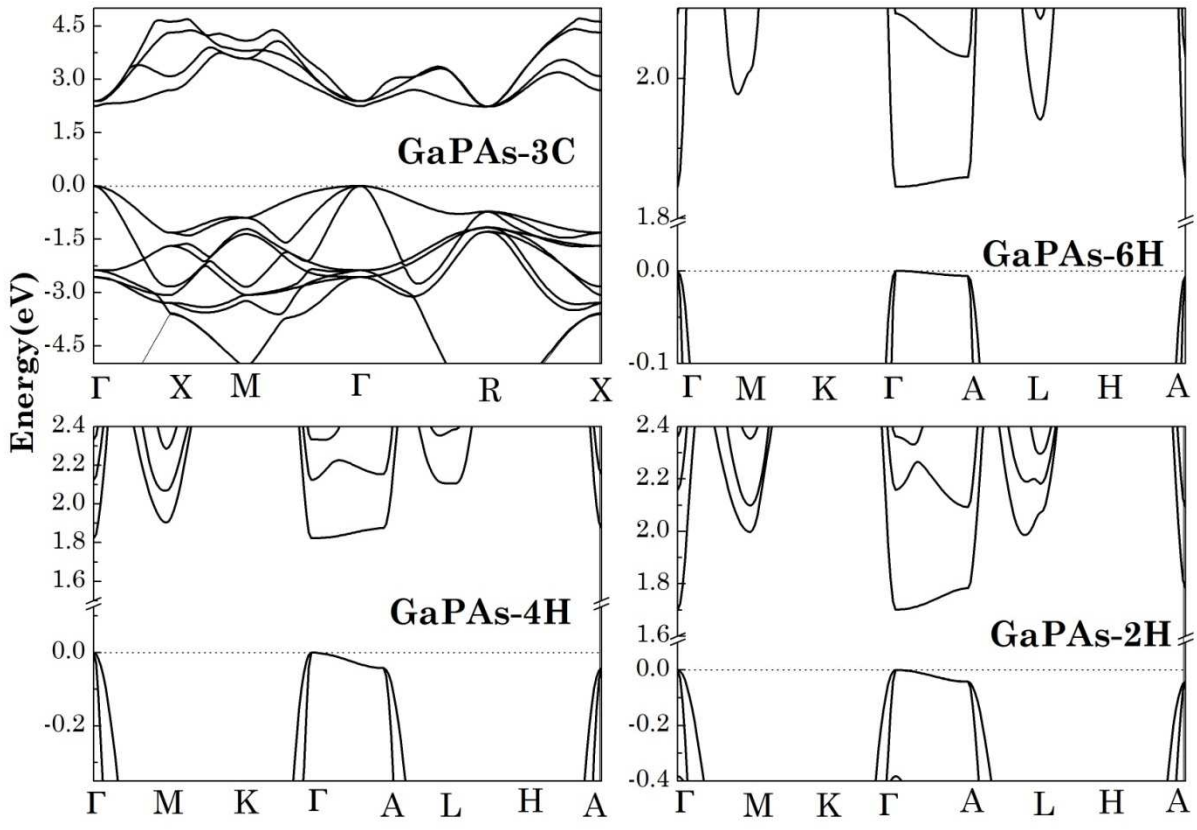
Energy(eV)
GaPAs-3C
Γ X M Γ R X
GaPAs-6H
Γ M K Γ A L H A
GaPAs-4H
Γ M K Γ A L H A
GaPAs-2H
Γ M K Γ A L H A

Figure 5

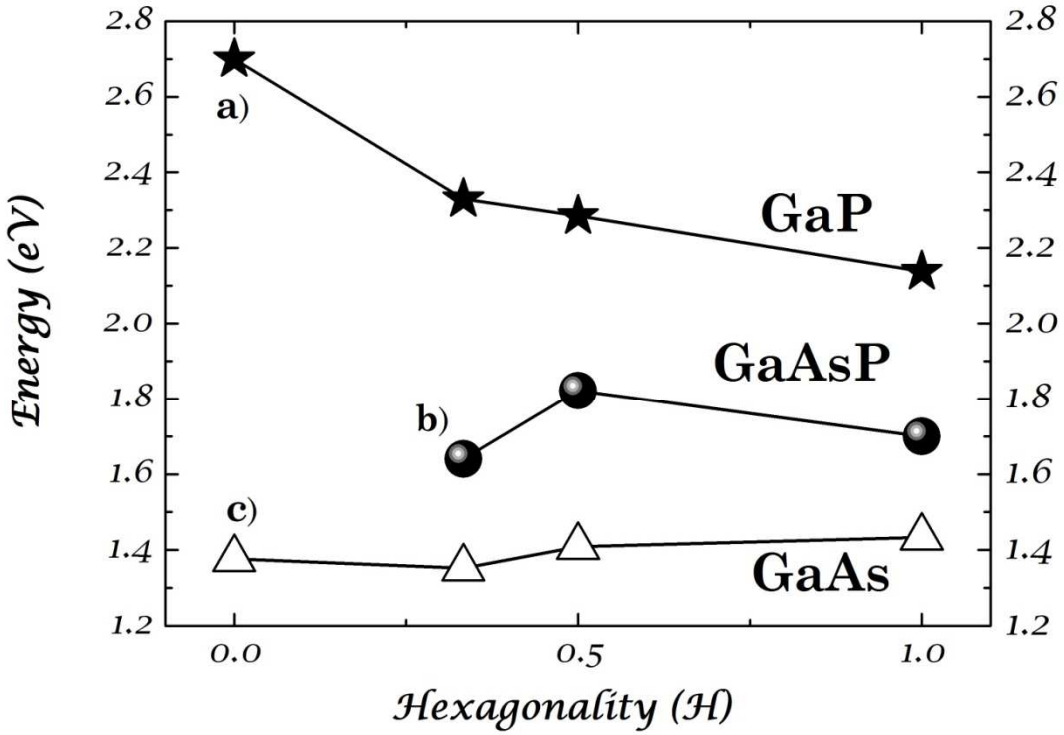
Energy (eV)
Hexagonality (H)
a)
b)
c)
GaP
GaAsP
GaAs
2.8
2.6
2.4
2.2
2.0
1.8
1.6
1.4
1.2
0.0
0.5
1.0